Predicting How Nanoconfinement Changes the Relaxation Time of a Supercooled Liquid

Trond S. Ingebrigtsen,[1,*] Jeffrey R. Errington,[2] Thomas M. Truskett,[3] and Jeppe C. Dyre[1]

[1]*DNRF Centre "Glass and Time," IMFUFA, Department of Sciences, Roskilde University, Postbox 260, DK-4000 Roskilde, Denmark*

[2]*Department of Chemical and Biological Engineering, University at Buffalo, The State University of New York, Buffalo, New York 14260, USA*

[3]*McKetta Department of Chemical Engineering and Institute for Theoretical Chemistry, University of Texas at Austin, Austin, Texas 78712, USA*

(Received 11 August 2013; published 2 December 2013)

The properties of nanoconfined fluids can be strikingly different from those of bulk liquids. A basic unanswered question is whether the equilibrium and dynamic consequences of confinement are related to each other in a simple way. We study this question by simulation of a liquid comprising asymmetric dumbbell-shaped molecules, which can be deeply supercooled without crystallizing. We find that the dimensionless structural relaxation times—spanning six decades as a function of temperature, density, and degree of confinement—collapse when plotted versus excess entropy. The data also collapse when plotted versus excess isochoric heat capacity, a behavior consistent with the existence of isomorphs in the bulk and confined states.

DOI: 10.1103/PhysRevLett.111.235901 PACS numbers: 65.20.Jk, 66.30.Pa, 68.15.+e

That confined liquids microscopically relax and flow with different characteristic time scales than bulk liquids is hardly surprising. Confining boundaries bias the spatial distribution of the constituent molecules and the ways by which those molecules can dynamically rearrange. These effects play important roles in the design of coatings, nanopatterning, and nanomanufacturing technologies [1,2]. As a result, they have already been experimentally characterized for a wide variety of material systems, including small-molecule fluids [3–10], polymers [11–16], ionic liquids [17], liquid crystals [18], and dense colloidal suspensions [19–23], and studied extensively via molecular simulations [22,24–31]. Recent reviews of confined-liquid behavior may be found in, e.g., Refs. [10,32].

Unfortunately, successful theories for predicting the dynamics of inhomogeneous fluids have been slower to emerge. Here, we explore the possibility of a novel approach for predicting how confinement affects the dynamics of viscous fluids. The central idea is motivated by the observation from molecular simulations that, under equilibrium conditions, key dimensionless "reduced" quantities for confined fluids closely correspond to those of homogeneous bulk fluids with the same excess entropy [33–37] (relative to an ideal gas at the same density and temperature). The excess entropy can be computed using Monte Carlo methods [36] or predicted from classical density-functional theories [35,38]. An open question is whether this observed correspondence between dynamics and excess entropy applies for fluids in deeply supercooled liquid states approaching the glass transition, where highly nontrivial dynamic effects of confinement are observed. Another open question is whether thermodynamic properties other than the excess entropy can be used to predict the dynamics in confinement.

To investigate these questions we study the behavior of a model glass former comprising asymmetric dumbbell-shaped molecules [39]. This model is perhaps the simplest single-component system that avoids freezing upon cooling or compression in confinement, allowing for a systematic comparison of the properties of supercooled states in both bulk and confined geometries. The latter is modeled as a slit pore, i.e., a sandwich geometry, using a 9-3 Lennard-Jones wall potential. The pore geometry is ideal for exploring the physics of confinement, which can be difficult to extract from experiments on porous materials that often have a complex distribution of pore sizes, geometries, and fluid-pore interactions [9,40]. The possible effects of corrugation and realistic pore geometries and interactions on scaling behavior are discussed in Refs. [34,36,41].

Molecular dynamics and Monte Carlo methods were used to simulate the model using high-speed graphics cards (GPUs [42]) for the former, obtaining for all state points consistent results from the two methods. Details of the model, simulations, units, etc., are provided in the Supplemental Material [43]. The longest production run was 4×10^9 time steps (approximately 360 GPU hours), requiring more than two months of prior equilibration. The main results obtained are proof of the existence of isomorphs in a strongly inhomogeneous fluid and, as a consequence of this, that the excess isochoric specific heat controls the relaxation time in the same sense as the excess entropy does.

We begin the investigation by studying in Fig. 1(a) the structural changes induced by the confining slit-pore geometry. This figure shows the molecular center-of-mass density profile in the direction normal to the walls of the slit pore (z direction). There are significant density

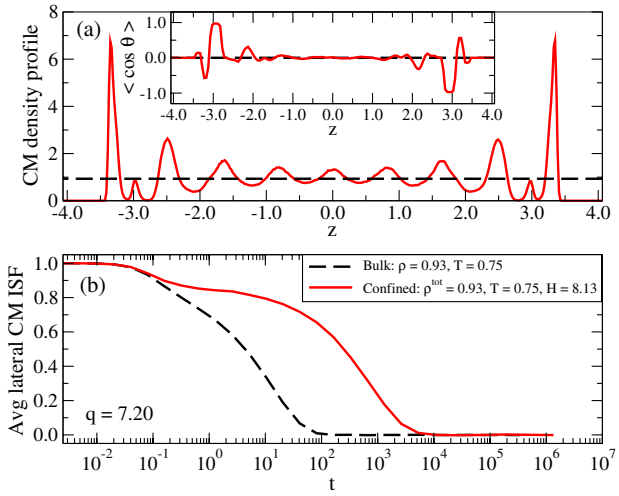

FIG. 1 (color online). Structure and dynamics of the asymmetric dumbbell model for the nanoscale-confined (full curve) and the bulk (dashed curve) liquid at the same temperature and average density. (a) The molecular center-of-mass density profile in the direction normal to the confining slit-pore walls (z direction); the inset gives the average orientation of the dumbbell molecules with respect to the z axis (see the Supplemental Material [43]). (b) The spatially averaged molecular center-of-mass incoherent intermediate scattering function for the wave vector $q = 7.20$ parallel to the walls of the slit pore.

oscillations, particularly close to the walls. Probing the average orientation of the dumbbell molecules with respect to the z axis (inset) reveals that preferred orientations emerge as the wall is approached. Both of these structural effects are absent in the bulk liquid, of course, and as shown in the Supplemental Material [43] they lead to a heterogeneous dynamics that is substantially slower near the walls. Figure 1(b) shows the spatially averaged dynamics in confinement and bulk liquid at the same temperature and average density; it is 2 orders of magnitude slower under confinement than in the bulk liquid phase. In fact, two-step relaxation—the hallmark of the supercooled viscous liquid state [44]—is seen in confinement but not at the corresponding bulk-liquid state point. The geometry thus has a pronounced effect on both structure and dynamics that cannot be accounted for by a trivial shifting or rescaling of the bulk data; this is observed in experimental realizations of similar systems [20,22,23].

To investigate whether the reduction in entropy upon confinement predicts the shift in mobility, we show in Fig. 2 the reduced spatially averaged structural relaxation time $\tilde{\tau}_\alpha$ in bulk and confinement as a function of the excess entropy $S_{\rm ex}$ (the relaxation time is determined from the molecular center-of-mass incoherent intermediate scattering function as described in detail in the Supplemental Material [43]). Two different versions of the excess entropy are shown. One uses the total slit-pore volume, and the other corrects for the nonaccessible volume close to the walls [36] (see the Supplemental Material [43]). Both versions capture well the changes in the dynamics induced by confinement.

If the structural relaxation time is plotted against the average density [see Figs. 3(a) and 3(b)], it is clear that density does not capture the changes that occur going into the highly viscous regime. As an example, comparing at the same average density $\rho^{\rm eff} = 1.05$ [see Fig. 3(b)], one would predict more than three decades too slow dynamics for a highly confined system (crosses) using the bulk behavior (vertical triangles); the opposite behavior is observed if the total density is used. The inset of Fig. 3(b) shows the effect that temperature has on the confined dynamics at conditions typical for this study. A super-Arrhenius behavior is observed at the lowest temperatures, consistent with experimental findings [45]. Figures 2 and 3 show that free-volume-type theories [46] cannot predict the dynamic consequences of confining the fluid, whereas the more microscopic, correlation-based measure $S_{\rm ex}$ can.

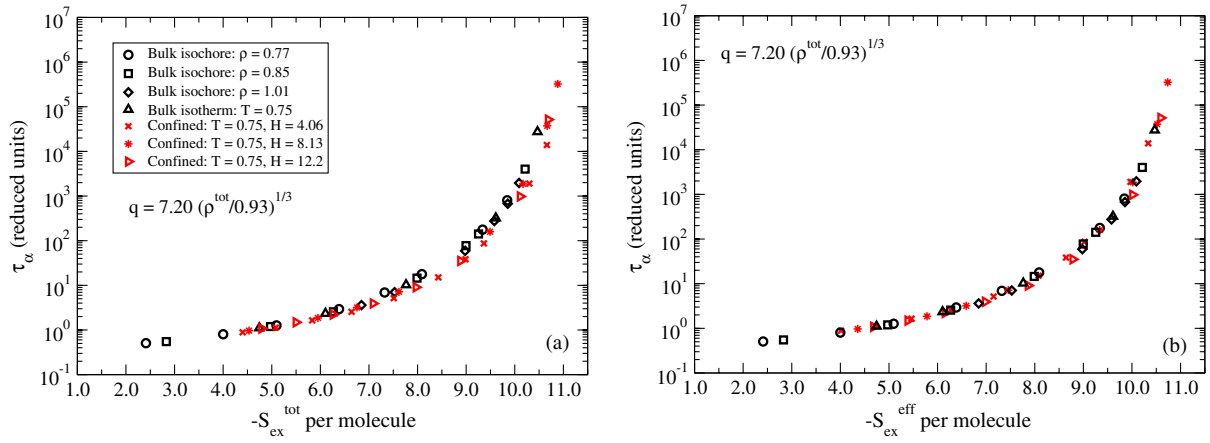

FIG. 2 (color online). The reduced spatially averaged structural relaxation time $\tilde{\tau}_\alpha$ in bulk and in confinement plotted (a) as a function of total excess entropy, and (b) as a function of effective excess entropy (see the Supplemental Material [43] for definitions). The bulk simulations have $\rho = 0.77$ and $0.14 \leq T \leq 12.5$; $\rho = 0.85$ and $0.25 \leq T \leq 12.5$; $\rho = 1.01$ and $0.69 \leq T \leq 2.00$.

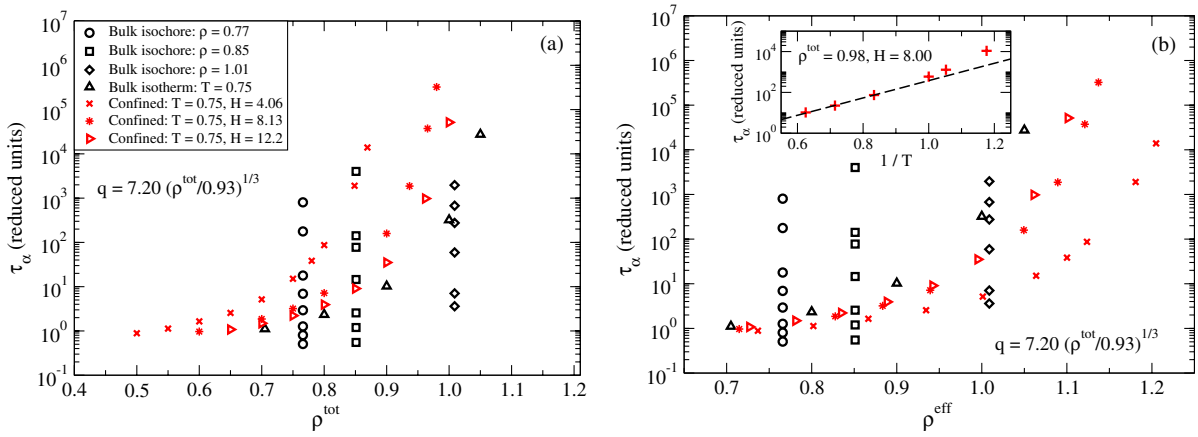

FIG. 3 (color online). The reduced spatially averaged structural relaxation time $\tilde{\tau}_\alpha$ in confinement and bulk plotted (a) as a function of average density $\rho^{\text{tot}} = N/(HA)$, and (b) as a function of effective average slit-pore density $\rho^{\text{eff}} = N/(H^{\text{eff}}A)$ (see the Supplemental Material [43]), where N is the number of molecules. The inset shows the effect that temperature has on the confined dynamics at conditions typical for this study. The bulk simulations have $\rho = 0.77$ and $0.14 \leq T \leq 12.5$; $\rho = 0.85$ and $0.25 \leq T \leq 12.5$; $\rho = 1.01$ and $0.69 \leq T \leq 2.00$.

We also probed a quantity that is much easier to calculate in simulations than S_{ex}, namely the excess isochoric heat capacity given by $C_V^{\text{ex}} = \langle(\Delta U)^2\rangle/k_B T^2$ (U is the potential energy, k_B is Boltzmann's constant, and T is the temperature). Figure 4 shows the structural relaxation time plotted as a function of C_V^{ex}. This quantity captures the dynamics of confinement over the full time span of six decades, although the collapse is not as good as for the excess entropy. Notably, the relaxation times of bulk and confined systems depend in the same way on C_V^{ex}, just as is the case for S_{ex}.

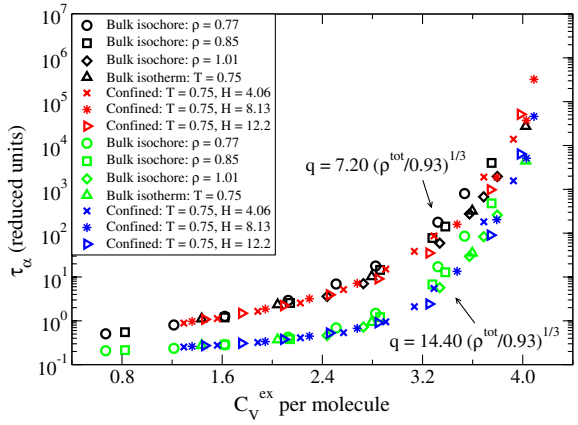

FIG. 4 (color online). The reduced spatially averaged structural relaxation time for the same wave vector q as studied previously, $\tilde{\tau}_\alpha$, in bulk and in confinement plotted as a function of the excess isochoric heat capacity per molecule. To a good approximation the heat capacity, like the entropy, tracks the dynamical changes induced by confinement. The bulk simulations have $\rho = 0.77$ and $0.14 \leq T \leq 12.5$; $\rho = 0.85$ and $0.25 \leq T \leq 12.5$; $\rho = 1.01$ and $0.69 \leq T \leq 2.00$. To demonstrate that the data collapse is not specific for one wave vector, the figure shows bulk and confinement data points for the double wave vector (see arrows).

According to Rosenfeld [47], the relaxation time is controlled by the excess entropy because a low excess entropy implies that many states are effectively rendered inaccessible, thereby increasing the relaxation time. But why does C_V^{ex} also predict the dynamics, why does density not work, and how general may one expect these findings to be? A possible explanation refers to the existence of isomorphs [48] in systems that display strong correlations between the equilibrium fluctuations of the potential energy U and the virial W in the NVT ensemble [49] ("Roskilde-simple" systems [50]). Recall that the instantaneous energy and pressure are each the sum of a trivial kinetic part and a configurational part. The latter are U and W, respectively. At any given state point the Pearson correlation coefficient R for the NVT thermal equilibrium fluctuations of U and W measures the strength of the correlations. Only inverse power-law fluids are perfectly correlating ($R = 1$), but many models [49], e.g., the Lennard-Jones liquid and some experimental liquids [51], have been shown to belong to the class of Roskilde-simple liquids defined by requiring $R \geq 0.90$ [49]. This class appears to include most or all van der Waals and metallic liquids, but exclude most or all covalently, hydrogen-bonding, or strongly ionic or dipolar liquids [49].

Roskilde-simple liquids are characterized by having good isomorphs [48]. An isomorph is a curve in the thermodynamic phase diagram along which structure and dynamics are invariant in reduced units; the excess entropy and the excess isochoric heat capacity are also invariant (but not the density). Since the reduced relaxation time is an isomorph invariant, both the excess entropy and the excess isochoric heat capacity predict the dynamics of Roskilde-simple liquids, whereas density does not.

In the bulk liquid phase the asymmetric dumbbell model is Roskilde simple [52]. To apply isomorph reasoning to a confined system, however, one needs to show that

isomorphs exist also for the nanoscale-confined liquid, which has entirely different physics. We document this in Fig. 5, where the molecular center-of-mass incoherent intermediate scattering function is shown along an isomorph and an isotherm. The dynamics is, to a good approximation, invariant along the isomorph, whereas along the isotherm one observes a substantial variation for less than half the density variation. We observed a similar behavior when probing the dynamics parallel to the walls at a fixed distance in reduced units from the wall (results not shown). Interestingly, the nanodynamics is isomorph invariant even though it is known to be spatially heterogeneous; this is because the entire spatial relaxation-time distribution in reduced units is predicted to be isomorph invariant.

The Supplemental Material [43] gives details on the definition of isomorphs in confinement and how they are generated in simulation. Briefly, the idea is the following. H is the distance between the two points where the wall potentials diverge, and A is the interfacial area of the slit-pore volume. Consider two state points (H_1, A_1, T_1) and (H_2, A_2, T_2) in the phase diagram of a confined liquid for which the state variables are related via $H_1^2/A_1 = H_2^2/A_2$, implying that a homogenous scaling of space maps slit pore 1 onto slit pore 2. These state points are isomorphic if the following holds: two microconfigurations, one of each state point, have proportional Boltzmann statistical probabilities whenever they for all molecules i have identical reduced coordinates, i.e., $\rho_{A_1}^{1/2} x_{\mathrm{CM},i}^{(1)} = \rho_{A_2}^{1/2} x_{\mathrm{CM},i}^{(2)}$, $\rho_{A_1}^{1/2} y_{\mathrm{CM},i}^{(1)} = \rho_{A_2}^{1/2} y_{\mathrm{CM},i}^{(2)}$, $\rho_{H_1} z_{\mathrm{CM},i}^{(1)} = \rho_{H_2} z_{\mathrm{CM},i}^{(2)}$ (in which $\rho_H \equiv N/H$, $\rho_A \equiv N/A$, and N is the number of molecules), as well as identical Eulerian angles. In particular, isomorphic state points are identical in their packing arrangements. If $\mathbf{R}$ is the collective configuration

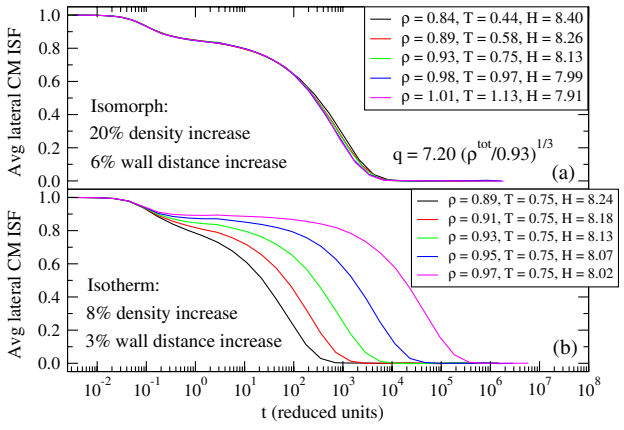

FIG. 5 (color online). The spatially averaged molecular center-of-mass incoherent intermediate scattering function as a function of reduced time for various state points of the asymmetric dumbbell model in confinement (a) along an isomorph, and (b) along an isotherm. The dynamics is to a good approximation invariant along the isomorph, but not along the isotherm even though it involves less than half of the density variation.

space coordinate this means that $\exp[-U(\mathbf{R}^{(1)})/k_B T_1] = C_{12} \exp[-U(\mathbf{R}^{(2)})/k_B T_2]$, where C_{12} depends only on the two thermodynamic state points, not on the microconfigurations. Taking the logarithm of this and rearranging, we get

$$U(\mathbf{R}^{(2)}) = \frac{T_2}{T_1} U(\mathbf{R}^{(1)}) + k_B T_2 \ln C_{12}. \quad (1)$$

Isomorphs are generated using this "direct isomorph check" [48] relation, where the walls of the slit pore follow the overall scaling in total density.

A very recently empirically established property of Roskilde-simple model liquids is that they obey Rosenfeld-Tarazona scaling ($C_V^{\mathrm{ex}} \propto T^{-2/5}$) significantly better than liquids in general [53]. From this one can understand why C_V^{ex} and S_{ex} both collapse the bulk data: integration of $C_V^{\mathrm{ex}} = (\partial S_{\mathrm{ex}}/\partial \ln T)_\rho \propto T^{-2/5}$ leads to $-S_{\mathrm{ex}} = (5/2)C_V^{\mathrm{ex}} + K(\rho)$. Isomorph invariance of S_{ex} and C_V^{ex} implies $K(\rho) = 0$, i.e., $-S_{\mathrm{ex}} = (5/2)C_V^{\mathrm{ex}}$. This is consistent with Figs. 2 and 4, but these figures tell us more, namely that both entropy and specific heat control the relaxation time of the bulk and the confined system in the same way.

Recently, Watanabe *et al.* [22] showed that the dynamics of a confined fluid system as a function of the distance to the walls can be described to a good approximation using the magnitude of the medium-range crystalline order [54–56]. A relation between the two-body excess entropy and the size of these regions has also been reported [55]. The two-body excess entropy is an isomorph invariant [48], so the results of Watanabe *et al.* confirm the existence of isomorphs in confinement.

Theories for confined liquids [57–60] must be consistent with the existence of isomorphs for Roskilde-simple fluids, a requirement that may be used as a "filter" when developing new approaches [48]: any theory for the reduced relaxation time—an isomorph invariant—must express this as a function of another isomorph invariant. Isomorphs are only relevant for fluids that are Roskilde simple [50], however. One should not expect dynamic or thermodynamic correlations to hold for strongly self-associating or network-forming liquids like water, which are not Roskilde simple, even in the bulk. Similarly, such correlations will not hold for certain idealized models, e.g., infinitely thin needles or crosses with ideal-gas-like static correlations [61], whose slow relaxations at high density are due to topological constraints, which, while not reflected in structure, hinder localized dynamic rearrangements. Finally, one expects such correlations to break down if length and energy scales of the fluid-wall interaction are substantially different from the fluid-fluid interaction or if the confining pores are very narrow. Evidence for the latter can be seen in Fig. 2 of the Supplemental Material [43].

To summarize, the excess or configurational entropy has for a long time been used to describe the relaxation time of

liquids [47,62,63] and more recently shown to work also for confined systems [33,64]. We demonstrated above a new controlling variable, the excess isochoric heat capacity, which is expected to apply for the fairly large class of liquids with strong correlations between virial and potential energy fluctuations in the *NVT* ensemble. We welcome new experimental as well as additional simulation studies of a wide spectrum of confined liquids to probe for the existence of isomorphs for confined liquids and, moreover, test the possible generality, beyond Roskilde-simple liquids, of this intriguing relation between static and dynamic properties.

The center for viscous liquid dynamics "Glass and Time" is sponsored by the Danish National Research Foundation (Contract No. DNRF61). T. M. T acknowledges support of the Welch Foundation (Contract No. F-1696) and the National Science Foundation (Contract No. CBET-1065357). J. R. E. acknowledges support of the National Science Foundation (Contract No. CHE-1012356). We also acknowledge the Texas Advanced Computing Center (TACC) at The University of Texas at Austin and the Center for Computational Research at the University at Buffalo for providing HPC resources that have contributed to the research results reported within this Letter. T. S. I. acknowledges useful discussions of confined-liquid behavior with Søren Toxvaerd.

*trond@ruc.dk

[1] B. Bhushan, J. N. Israelachvili, and U. Landman, Nature (London) **374**, 607 (1995).
[2] G. M. Whitesides, Nature (London) **442**, 368 (2006).
[3] J. M. Drake and J. Klafter, Phys. Today **43**, No. 5, 46 (1990).
[4] S. Granick, Science **253**, 1374 (1991).
[5] D. Morineau, Y. Xia, and C. Alba-Simionesco, J. Chem. Phys. **117**, 8966 (2002).
[6] C. L. Jackson and G. B. McKenna, J. Non-Cryst. Solids **131-133**, 221 (1991).
[7] V. Teboul and C. Alba-Simionesco, Chem. Phys. **317**, 245 (2005).
[8] M. Alcoutlabi and G. B. McKenna, J. Phys. Condens. Matter **17**, R461 (2005).
[9] B. Coasne, C. Alba-Simionesco, F. Audonnet, G. Dosseh, and K. E. Gubbins, Phys. Chem. Chem. Phys. **13**, 3748 (2011).
[10] R. Richert, Annu. Rev. Phys. Chem. **62**, 65 (2011).
[11] J. L. Keddie, R. A. L. Jones, and R. A. Cory, Europhys. Lett. **27**, 59 (1994).
[12] A. Serghei, M. Tress, and F. Kremer, Macromolecules **39**, 9385 (2006).
[13] J. A. Forrest and K. Dalnoki-Veress, Adv. Colloid Interface Sci. **94**, 167 (2001).
[14] C. J. Ellison and J. M. Torkelson, Nat. Mater. **2**, 695 (2003).
[15] P. Rittigstein, R. D. Priestley, L. J. Broadbelt, and J. M. Torkelson, Nat. Mater. **6**, 278 (2007).
[16] K. Paeng, R. Richert, and M. D. Ediger, Soft Matter **8**, 819 (2012).
[17] C. Iacob, J. R. Sangoro, W. K. Kipnusu, R. Valiullin, J. Kärger, and F. Kremer, Soft Matter **8**, 289 (2012).
[18] Q. Ji, R. Lefort, A. Ghoufi, and D. Morineau, Chem. Phys. Lett. **482**, 234 (2009).
[19] C. R. Nugent, K. V. Edmond, H. N. Patel, and E. R. Weeks, Phys. Rev. Lett. **99**, 025702 (2007).
[20] H. B. Eral, D. van den Ende, F. Mugele, and M. H. G. Duits, Phys. Rev. E **80**, 061403 (2009).
[21] V. N. Michailidou, G. Petekidis, J. W. Swan, and J. F. Brady, Phys. Rev. Lett. **102**, 068302 (2009).
[22] K. Watanabe, T. Kawasaki, and H. Tanaka, Nat. Mater. **10**, 512 (2011).
[23] K. V. Edmond, C. R. Nugent, and E. R. Weeks, Phys. Rev. E **85**, 041401 (2012).
[24] T. Fehr and H. Löwen, Phys. Rev. E **52**, 4016 (1995).
[25] J. A. Torres, P. F. Nealey, and J. J. de Pablo, Phys. Rev. Lett. **85**, 3221 (2000).
[26] P. Scheidler, W. Kob, and K. Binder, J. Phys. IV (France) **10**, 33 (2000).
[27] F. W. Starr, T. B. Schrøder, and S. C. Glotzer, Macromolecules **35**, 4481 (2002).
[28] A. R. C. Baljon, M. H. M. V. Weert, R. B. DeGraaff, and R. Khare, Macromolecules **38**, 2391 (2005).
[29] J. Kurzidim, D. Coslovich, and G. Kahl, Phys. Rev. Lett. **103**, 138303 (2009).
[30] F. W. Starr and J. F. Douglas, Phys. Rev. Lett. **106**, 115702 (2011).
[31] B. A. P. Betancourt, J. F. Douglas, and F. W. Starr, Soft Matter **9**, 241 (2013).
[32] C. Alba-Simionesco, B. Coasne, G. Dosseh, G. Dudziak, K. E. Gubbins, R. Radhakrishnan, and M. Sliwinska-Bartkowiak, J. Phys. Condens. Matter **18**, R15 (2006).
[33] J. Mittal, J. R. Errington, and T. M. Truskett, Phys. Rev. Lett. **96**, 177804 (2006).
[34] J. Mittal, J. R. Errington, and T. M. Truskett, J. Phys. Chem. B **111**, 10054 (2007).
[35] G. Goel, W. P. Krekelberg, M. J. Pond, J. Mittal, V. K. Shen, J. R. Errington, and T. M. Truskett, J. Stat. Mech., 4 (2009) P04006.
[36] R. Chopra, T. M. Truskett, and J. R. Errington, Phys. Rev. E **82**, 041201 (2010).
[37] B. J. Borah, P. K. Maiti, C. Chakravarty, and S. Yashonath, J. Chem. Phys. **136**, 174510 (2012).
[38] H. S. Gulati and C. K. Hall, J. Chem. Phys. **107**, 3930 (1997).
[39] T. B. Schrøder, U. R. Pedersen, N. P. Bailey, S. Toxvaerd, and J. C. Dyre, Phys. Rev. E **80**, 041502 (2009).
[40] M. Schoeffel, N. Brodie-Linder, F. Audonnet, and C. Alba-Simionesco, J. Mater. Chem. **22**, 557 (2012).
[41] W. P. Krekelberg, V. K. Shen, J. R. Errington, and T. M. Truskett, J. Chem. Phys. **135**, 154502 (2011).
[42] See http://rumd.org.
[43] See Supplemental Material http://link.aps.org/supplemental/10.1103/PhysRevLett.111.235901 for details of the model and simulations, the definition of isomorphs in confinement and their generation in simulations, as well as the parameters used in the analytical methods.
[44] P. G. Debenedetti and F. H. Stillinger, Nature (London) **410**, 259 (2001).

[45] G. Dosseh, C. L. Quellec, N. Brodie-linder, C. Alba-simionesco, W. Haeussler, and P. Levitz, J. Non-Cryst. Solids **352**, 4964 (2006).
[46] M. H. Cohen and G. S. Grest, Phys. Rev. B **20**, 1077 (1979).
[47] Y. Rosenfeld, Phys. Rev. A **15**, 2545 (1977).
[48] N. Gnan, T. B. Schrøder, U. R. Pedersen, N. P. Bailey, and J. C. Dyre, J. Chem. Phys. **131**, 234504 (2009).
[49] N. P. Bailey, U. R. Pedersen, N. Gnan, T. B. Schrøder, and J. C. Dyre, J. Chem. Phys. **129**, 184507 (2008).
[50] T. S. Ingebrigtsen, T. B. Schrøder, and J. C. Dyre, Phys. Rev. X **2**, 011011 (2012).
[51] D. Gundermann, U. R. Pedersen, T. Hecksher, N. P. Bailey, B. Jakobsen, T. Christensen, N. B. Olsen, T. B. Schrøder, D. Fragiadakis, R. Casalini, C. M. Roland, J. C. Dyre, and K. Niss, Nat. Phys. **7**, 816 (2011).
[52] T. S. Ingebrigtsen, T. B. Schrøder, and J. C. Dyre, J. Phys. Chem. B **116**, 1018 (2012).
[53] T. S. Ingebrigtsen, A. A. Veldhorst, T. B. Schrøder, and J. C. Dyre, J. Chem. Phys. **139**, 171101 (2013).
[54] H. Shintani and H. Tanaka, Nat. Phys. **2**, 200 (2006).
[55] T. Kawasaki, T. Araki, and H. Tanaka, Phys. Rev. Lett. **99**, 215701 (2007).
[56] M. Leocmach and H. Tanaka, Nat. Commun. **3**, 974 (2012).
[57] V. Krakoviack, Phys. Rev. Lett. **94**, 065703 (2005).
[58] G. Biroli, J.-P. Bouchaud, K. Miyazaki, and D. R. Reichman, Phys. Rev. Lett. **97**, 195701 (2006).
[59] S. Lang, V. Botan, M. Oettel, D. Hajnal, T. Franosch, and R. Schilling, Phys. Rev. Lett. **105**, 125701 (2010).
[60] S. Lang, R. Schilling, V. Krakoviack, and T. Franosch, Phys. Rev. E **86**, 021502 (2012).
[61] W. van Ketel, C. Das, and D. Frenkel, Phys. Rev. Lett. **94**, 135703 (2005).
[62] G. Adam and J. H. Gibbs, J. Chem. Phys. **43**, 139 (1965).
[63] X. Ma, W. Chen, Z. Wang, Y. Peng, Y. Han, and P. Tong, Phys. Rev. Lett. **110**, 078302 (2013).
[64] C. Cammarota, G. Gradenigo, and G. Biroli, Phys. Rev. Lett. **111**, 107801 (2013).